Inorg. Chem. **2005**, *44*, 5641–5648

Mesoporous Silica-Supported Uranyl: Synthesis and Photoreactivity

Jennifer A. Nieweg, Kelemu Lemma, Brian G. Trewyn, Victor S.-Y. Lin,* and Andreja Bakac*

Ames Laboratory and Chemistry Department, Iowa State University, Ames, Iowa 50011

Received January 26, 2005

A mesoporous silica-supported uranyl material ($U_{aq}O_2^{2+}$–silica) was prepared by a co-condensation method. Our approach involves an $I^-M^+S^-$ scheme, where the electrostatic interaction between the anionic inorganic precursor (I^-), surfactant (S^-), and cationic mediator (M^+) provides the basis for the stability of the composite material. The synthesis was carried out under acidic conditions, where the anionic sodium dodecyl sulfate provided the template for the uranyl cation and silicate to condense. Excitation with visible or near-UV light of aqueous suspensions of $U_{aq}O_2^{2+}$–silica generates an excited state that decays with $k_0 = 1.5 \times 10^4$ s^{-1}. The reaction of the excited state with aliphatic alcohols exhibits kinetic saturation and concentration-dependent kinetic isotope effects. For 2-propanol, the value of $k_{C_3H_7OH}/k_{C_3D_7OH}$ decreases from 2.0 at low alcohol concentrations to 1.0 in the saturation regime at high alcohol concentrations. Taken together, the data describe a kinetic system controlled by chemical reaction at one extreme and diffusion at the other. At low [alcohol], the second-order rate constants for the reaction of silica–$*U_{aq}O_2^{2+}$ with methanol, 2-propanol, 2-butanol, and 2-pentanol are comparable to the rate constants obtained for these alcohols in homogeneous aqueous solutions containing H_3PO_4. Under slow steady-state photolysis in O_2-saturated suspensions, $U_{aq}O_2^{2+}$–silica acts as a photocatalyst for the oxidation of alcohols with O_2.

Introduction

The extraordinary chemical and physical properties of excited uranyl ions have been uncovered, reported,[1−8] and reviewed over the past several decades.[9−13] $*U_{aq}O_2^{2+}$, easily detected by its intense green luminescence,[11] is a potent and long-lived oxidant for organic and inorganic substrates.[10] In solution studies, both stoichiometric[10] and catalytic[14−17] reactions have been carried out, the latter taking advantage of reasonably rapid oxidation of the one-electron-reduced species, $U_{aq}O_2^{+}$, by molecular oxygen and hydrogen peroxide.[18] A typical catalytic reaction utilizing O_2 as the active oxidant, shown for 2-propanol (2-PrOH) in Scheme 1, is initiated by hydrogen atom abstraction to generate radicals, which are oxidized further to stable products. In the final step, $U_{aq}O_2^{2+}$ is regenerated by oxidation of $U_{aq}O_2^{+}$ with O_2, H_2O_2, and/or various oxygen radicals.[14]

Scheme 1

$$U_{aq}O_2^{2+} + h\nu \rightarrow *U_{aq}O_2^{2+}$$

$$*U_{aq}O_2^{2+} + (CH_3)_2CHOH \rightarrow U_{aq}O_2^{+} + (CH_3)_2C^{\bullet}OH$$

$$(CH_3)_2C^{\bullet}OH \xrightarrow{O_2,\ U(VI)} (CH_3)_2CO$$

$$2U_{aq}O_2^{+} + O_2\,(+2H+) \rightarrow 2U_{aq}O_2^{2+} + H_2O_2$$

* To whom correspondence should be addressed. E-mail: vsylin@iastate.edu (V.S.-Y.L.), bakac@ameslab.gov (A.B.).

(1) Matsushima, R. *J. Am. Chem. Soc.* **1972**, *94*, 6010−6016.
(2) Burrows, H. D.; Formosinho, S. J. *J. Chem. Soc., Faraday Trans. 2* **1977**, *73*, 201−208.
(3) Marcantonatos, M. D.; Pawlowska, M. M. *J. Chem. Soc., Faraday Trans. 1* **1989**, *85*, 2481−2498.
(4) Yamaguchi, T.; Harada, M.; Park, Y.-Y.; Tomiyasu, H. *J. Chem. Soc., Faraday Trans.* **1990**, *86*, 1621−1622.
(5) Park, Y.-Y.; Tomiyasu, H. *J. Photochem. Photobiol. A* **1992**, *64*, 25−33.
(6) Sarakha, M.; Bolte, M.; Burrows, H. D. *J. Phys. Chem. A* **2000**, *104*, 3142−3149.
(7) Park, Y.-Y.; Sakai, Y.; Abe, R.; Ishii, T.; Harada, M.; Kojima, T.; Tomiyasu, H. *J. Chem. Soc., Faraday Trans.* **1990**, *86*, 55−60.
(8) Azenha, M. E. D. G.; Burrows, H. D.; Formosinho, S. J.; Miguel, M. G. M.; Daramanyan, A. P.; Khudyakov, I. V. *J. Luminescence* **1991**, *48−49*, 522−526.
(9) Jorgensen, C. K.; Reisfeld, R. *Struct. Bonding (Berlin)* **1982**, *50*, 121−171.
(10) Hoffman, M. Z.; Bolletta, F.; Moggi, L.; Hug, G. L. *J. Phys. Chem. Ref. Data* **1989**, *18*, 219−543.
(11) Balzani, V.; Bolletta, F.; Gandolfi, M. T.; Maestri, M. *Top. Curr. Chem.* **1978**, *75*, 1−64.
(12) Burrows, H. D.; Kemp, T. J. *Chem. Soc. Rev.* **1974**, *3*, 139−165.
(13) Buchachenko, A. L.; Khudyakov, I. V. *Acc. Chem. Res.* **1991**, *24*, 177−183.
(14) Mao, Y.; Bakac, A. *J. Phys. Chem.* **1995**, *100*, 4219−4223.
(15) Mao, Y.; Bakac, A. *Inorg. Chem.* **1996**, *35*, 3925−3930.
(16) Mao, Y.; Bakac, A. *J. Phys. Chem. A* **1997**, *101*, 7929−7933.
(17) Wang, W.-D.; Bakac, A.; Espenson, J. H. *Inorg. Chem.* **1995**, *34*, 6034−6039.
(18) Bakac, A.; Espenson, J. H. *Inorg. Chem.* **1995**, *34*, 1730−1735.

10.1021/ic050130e CCC: $30.25
Published on Web 07/14/2005

$U_{aq}O_2^{2+}$ supported on silica,[19] zeolites,[20−23] clays,[22,24] Nafion membranes,[25] and glasses[26] retains the basic photochemical and photophysical features of the solution species, with additional inevitable complexities arising from the heterogeneity of the environment. The excited states of the supported uranyl are typically more persistent[19,27] and the decay kinetics more complex[21,24,27] than those of solution ions, indicating the presence of several uranyl species and/or crystallographic sites in the supported materials. In the absence of an obvious mechanism for rapid equilibration, the various hydrolytic forms[28] of monomeric and polymeric uranyl trapped on the solid support must be decaying and reacting with substrates virtually independently of each other.

Photoexcited supported uranyl has been shown to react with some organic substrates,[19,21,22,24,26] although the kinetics were usually slower than those in solution. The lower reactivity is in part offset by the longer lifetimes, which allowed the catalytic oxidation of alcohols to be successful in several instances.[19,21,22,24] The exceptionally rapid quenching of $*U_{aq}O_2^{2+}$ on Nafion membranes by alcohols has been reported, but the products or the quenching mechanism have not been addressed.[25]

Successful oxidation of organic substrates with O_2 or H_2O_2, photocatalyzed or photoinitiated by $U_{aq}O_2^{2+}$ under heterogeneous conditions, would be a great step forward in the search for efficient and selective oxidative catalytic systems. The promise of at least some selectivity came in our earlier solution chemistry, which generated fewer products[17] than is typical for free-radical reactions, such as those based on Fenton or radiation-induced chemistry. Similarly, $U_{aq}O_2^{2+}$ in clay pillars was found to be more selective than some other supported forms, suggesting that the proper choice of support may lead to even greater selectivity for desired products.[22]

These observations and ideas encouraged us to synthesize mesoporous silica-supported uranyl with well-defined uranyl sites and to explore the behavior of these materials in photoassisted oxidation of organic materials. Mesoporous hosts that contain uranyl ions[29−32] and oxides[33,34] have been prepared by a variety of approaches, including hydrothermal synthesis,[29,32] wet impregnation,[32,34] direct template ion-exchange,[30,31,34a] and block copolymer[33] templating methods. The majority of these syntheses employ cationic surfactants[29−32,34] as templates for the anionic silica to condense under basic conditions by following the I^-S^+ (where I is the inorganic precursor and S^+ is the surfactant template) synthetic method. The uranyl precursor is incorporated into the structure during this condensation or is integrated after the silica material has been established. In contrast to the I^-S^+ method, Zhang et al.[33] recently developed a $I^+M^-S^+$ method, where a protonated block copolymer (S^+) could support the positively charged inorganic oxide (I^+) in the presence of an anionic mediator ion (M^-). Materials synthesized by these methods relied on calcination to remove the surfactant template and ensure the incorporation of the uranyl ions/oxides. This high-temperature thermal treatment yielded uranium oxide species, such as U_3O_8, that have no photocatalytic properties.

To preserve the photocatalytic property of $U_{aq}O_2^{2+}$ in the mesoporous host, we have developed a new synthetic method following an $I^-M^+S^-$ scheme, where the electrostatic interaction between the anionic inorganic precursor (I^-), surfactant (S^-), and cationic mediator (M^+) provides the basis for the stability of the material. Herein, we report a co-condensation method based on the above templating scheme for the synthesis of $U_{aq}O_2^{2+}$-incorporated mesoporous silica materials. The synthesis is carried out under acidic conditions, where the anionic sodium dodecyl sulfate (SDS) surfactant provides the template for the uranyl cation and silicate to condense.

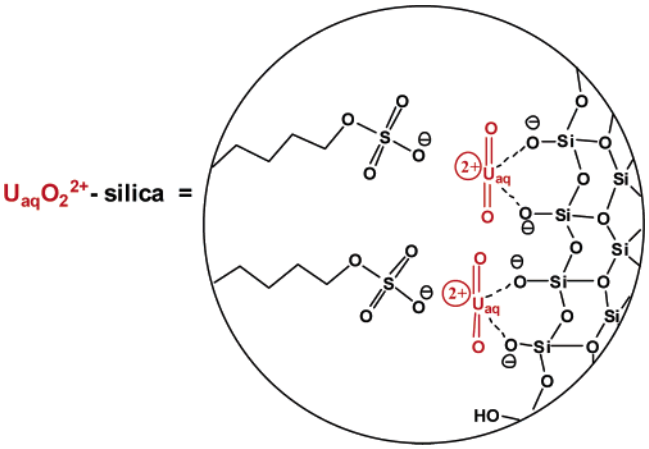

Experimental Section

Materials. Tetraethyl orthosilicate (TEOS, Aldrich), *n*-cetyltrimethylammonium bromide (Aldrich), sodium dodecyl sulfate (SDS, Fisher), and uranyl nitrate hexahydrate (Ladd Research Industries) were used as received. Alcohols (Fisher and Aldrich), deuterium oxide (99.9% D, Aldrich), and silica gel (7−230 mesh, 100 Å,

(19) Wheeler, J.; Thomas, J. K. *J. Phys. Chem.* **1984**, *88*, 750−754.
(20) Yang, C.-L.; El-Sayed, M. A.; Suib, S. L. *J. Phys. Chem.* **1987**, *91*, 4440−4443.
(21) Suib, S. L.; Kostapapas, A.; Psaras, D. *J. Am. Chem. Soc.* **1984**, *106*, 1614−1620.
(22) Suib, S. L.; Tanguay, J. F.; Occelli, M. L. *J. Am. Chem. Soc.* **1986**, *108*, 6972−6977.
(23) Suib, S. L.; Carrado, K. A. *Inorg. Chem.* **1985**, *24*, 200−202.
(24) Suib, S. L.; Carrado, K. A. *Inorg. Chem.* **1985**, *24*, 863−867.
(25) Watanabe, C. N.; Gehlen, M. H. *J. Photochem. Photobiol., A* **2003**, *156*, 65−68.
(26) Dai, S.; Metcalf, D. H.; Cul, G. D. D.; Toth, L. M. *Inorg. Chem.* **1996**, *35*, 7786−7790.
(27) Lopez, M.; Birch, D. J. S. *Analyst* **1996**, *121*, 905−908.
(28) Zanonato, P. L.; Bernardo, P. D.; Bismondo, A.; Liu, G.; Chen, X.; Rao, L. *J. Am. Chem. Soc.* **2004**, *126*, 5515−5522.
(29) Tismaneanu, R.; Ray, B.; Khalfin, R.; Semiat, R.; Eisen, M. S. *J. Mol. Catal. A: Chem.* **2001**, *171*, 229−241.
(30) Vidya, K.; Dapurkar, S. E.; Selvam, P.; Badamali, S. K.; Gupta, N. M. *Microporous Mesoporous Mater.* **2001**, *50*, 173−179.
(31) (a) Vidya, K.; Dapurkar, S. E.; Selvam, P.; Badamali, S. K.; Kumar, D.; Gupta, N. M. *J. Mol. Catal. A: Chem* **2002**, *181*, 91−97. (b) Krishna, V.; Kamble, V. S.; Selvam, P.; Gupta, N. M. *Catal. Lett.* **2004**, *98*, 113−116.
(32) Kumar, D.; Pillai, K. T.; Sudersanan, V.; Dey, G. K.; Gupta, N. M. *Chem. Mater.* **2003**, *15*, 3859−3865 and references therein.
(33) Zhang, Z. T.; Konduru, M.; Dai, S.; Overbury, S. H. *Chem. Commun.* **2002**, 2406−2407 and references therein.
(34) (a) Kumar, D.; Dey, G. K.; Gupta, N. M. *Phys. Chem. Chem. Phys.* **2003**, *5*, 5477−5484. (b) Kumar, D.; Bera, S.; Tripathi, A. K.; Dey, G. K.; Gupta, N. M. *Microporous Mesoporous Mater.* **2003**, *66*, 157−167.

Merck) were used as received. Nanopure water was obtained by passing distilled water through a Millipore Milli-Q water purification system (for kinetics) or through a Barnstead E-Pure system (for synthesis).

Preparation of Mesoporous $U_{aq}O_2^{2+}$−Silica. The material was prepared in a co-condensation reaction between the anionic surfactant SDS, the uranyl ion precursor uranyl nitrate hexahydrate, and the silica precursor TEOS under acidic conditions.

The synthesis entailed reactants in a molar ratio of 10:0.6:0.2:71.5:498.8 TEOS/$UO_2(NO_3)_2$·$6H_2O$/SDS/HCl/H_2O. SDS (159 mg, 5.5×10^{-4} mol) was dissolved in 12 mL of Nanopure water. After dissolution, HCl(aq) (2.00 M, 94.7 mL) was added to this SDS solution, and the solution temperature was adjusted to 35 °C. The silica precursor TEOS (5.92 mL, 2.7×10^{-2} mol) and an aqueous uranyl nitrate solution (0.13 M, 11.8 mL) were introduced dropwise simultaneously. The mixture was stirred at 35 °C for 24 h to yield a cloudy yellow solution. After 24 h, the temperature was increased to 100 °C and the stirring was stopped. The solution was heated at 100 °C for 36 h to yield a yellow gel, which was filtered and subsequently washed with Nanopure water and methanol (MeOH). After 5 h of vacuum-drying with stirring at 80 °C, a yellow powder was obtained. The powder was lyophilized for 12 h prior to use in kinetic experiments.

Instrumental Conditions and Parameters for $U_{aq}O_2^{2+}$−Silica Catalyst Characterization. Powder X-ray diffraction data were collected on a Scintag XRD 2000 X-ray diffractometer using Cu Kα radiation. Diffraction patterns were obtained at higher 2θ values (10−80°) to verify the absence of uranium oxide clusters. The scan speed was 0.04° min^{-1}, and the step size was 0.02°.

Nitrogen adsorption and desorption isotherm, surface area, and median pore diameter were measured using a Micrometrics ASAP2000 sorptometer. The sample preparation included degassing at 90 °C for approximately 4 h. Nitrogen adsorption and desorption isotherms were obtained at −196 °C. Specific surface areas and pore size distributions were calculated using the Brunauer−Emmett−Teller (BET) and Barrett−Joyner−Halenda (BJH) methods, respectively.

The particle morphology of the material was determined with scanning electron microscopy (SEM) and transmission electron microscopy (TEM). The SEM spectra were obtained using a JEOL 840A scanning electron microscope with 20-kV accelerating voltage and 0.005 nA of beam current for imaging. For TEM analysis, samples were microtomed using a Reichert Ultracut T ultramicrotome. Samples were prepared for microtoming by embedding samples in EPON epoxy resin using EmBed 812. The embedding suspension was cured twice for 24 h at 60 and 70 °C. The embedding block was microtomed to obtain thin sections of 80−100-nm thickness by using a Diatome diamond knife. The sections were mounted on lacey carbon film-coated 400-mesh Cu grid. The TEM image was recorded using a Philips CM-30 TEM operated at 300 kV.

Spectroscopic Measurements. Emission spectra were recorded in water with a Fluoromax-2 (Instruments SA, Inc.) spectrofluorimeter. The excitation wavelength was 420 nm. A Shimadzu 3101 PC spectrophotometer and a Bruker DRX 400-MHz NMR spectrometer were used for UV−vis and ^{1}H NMR measurements, respectively.

Kinetics. The luminescence decay of $*U_{aq}O_2^{2+}$−silica was monitored by laser flash photolysis using a flashlamp-pumped Phase-R model DL-1100 dye laser[35] (λ_{exc} = 490 nm). Small volumes of alcohols were injected into a 3 mL of water/$U_{aq}O_2^{2+}$−silica (10 mg) mixture, and the luminescence decay was followed at 515 nm. Data analyses were performed by use of a KaleidaGraph 3.09 PC software.

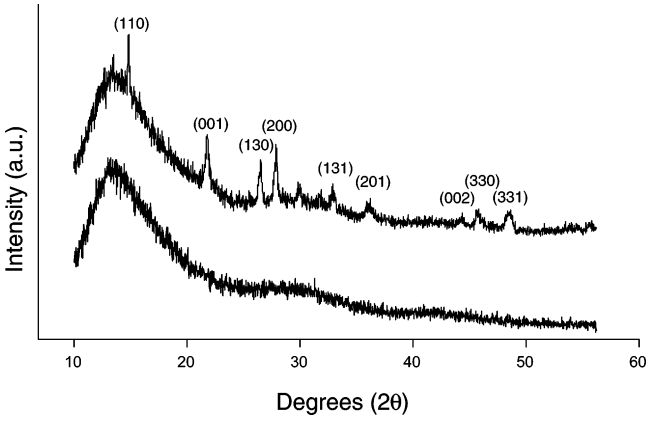

Figure 1. High-angle powder XRD pattern of $U_{aq}O_2^{2+}$−silica. The bottom spectrum shows the as-synthesized material. The top spectrum, obtained after calcination at 800 °C, exhibits diffraction peaks of U_3O_8 clusters.

Photooxidation of Alcohols. To 20 mg of $U_{aq}O_2^{2+}$−silica in 3 mL of D_2O in a 1-cm rectangular fluorescence cell was added 40 μL of 0.148 M NaOD. The pH of such solutions was around 5. The desired amount of neat alcohol was added, and the cell was immersed into an ice-cold water bath. The mixture was stirred on a magnetic stirrer and irradiated for variable periods of time using a Sperti Del Sol sunlamp, λ_{exc} = 366 nm (∼75%) and 313 nm (∼25%). Every 10 min, the irradiation was interrupted and the reaction mixture reoxygenated by a slow stream of O_2 through the ice-cooled solution. After photolysis, the mixture was centrifuged and the supernatant liquid filtered through a 0.22-μm filter. The product yields were determined by ^{1}H NMR.

Results

Synthesis and Characterization of Mesoporous $U_{aq}O_2^{2+}$−SiO_2. Electrostatic attractions provide the basis for the stability of the mesoporous $U_{aq}O_2^{2+}$−SiO_2. In the $I^-M^+S^-$ scheme employed, the surfactant plays a role not only in the templating of the structure but also in the stability of the material and the loading of uranyl ions. In contrast to calcination-based methods, in the present case the surfactant does not need to be removed to allow uranyl ions to adhere to the silica.

As shown in the top spectrum of Figure 1, the high-angle powder XRD pattern of the mesoporous $U_{aq}O_2^{2+}$−SiO_2 material that was calcined at 800 °C for 5 h in the open air showed distinct diffraction peaks of U_3O_8 clusters. This material did not show any photocatalytic activity. In contrast, the XRD spectrum (bottom, Figure 1) of the mesoporous $U_{aq}O_2^{2+}$−SiO_2 material without calcination treatment exhibited no undesired uranium oxide diffraction peaks at high angles, indicating the absence of U_3O_8 clusters. The broad peak around 23° observed in both spectra is characteristic of amorphous silica and is seen in many mesoporous silica systems. Our result is consistent with those of recent literature reports, where high-temperature calcination of silica-supported uranyl complexes indeed resulted in the formation of uranium oxide clusters.[33,34] The low-angle XRD measurement of the uncalcined mesoporous $U_{aq}O_2^{2+}$−SiO_2 material exhib-

(35) Melton, J. D.; Espenson, J. H.; Bakac, A. *Inorg. Chem.* **1986**, *25*, 4104−4108.

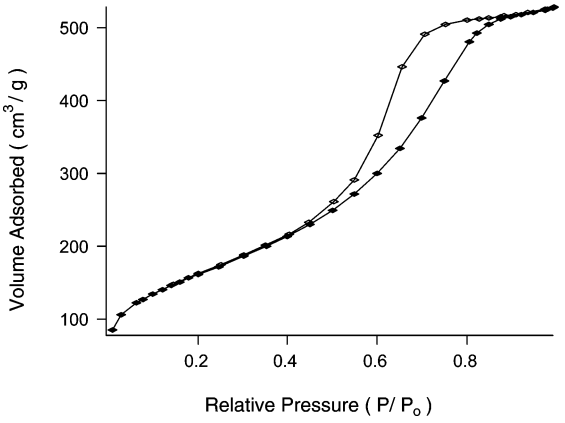

Figure 2. Nitrogen sorption isotherm of $U_{aq}O_2^{2+}$−silica.

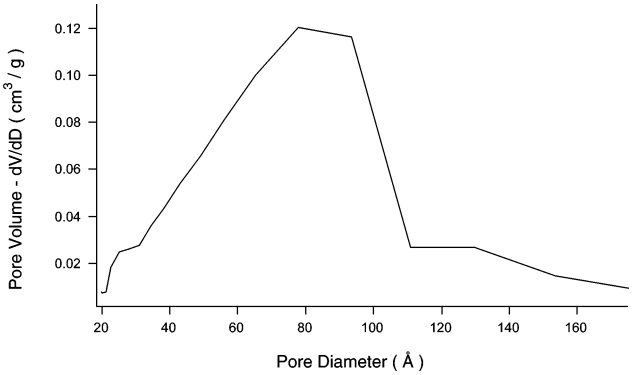

Figure 3. BJH pore size distribution of $U_{aq}O_2^{2+}$−silica.

ited only a shoulder below 1.5°, indicating a distorted mesoporous structure.

As depicted in Figure 2, the N_2 adsorption/desorption isotherm of the mesoporous $U_{aq}O_2^{2+}$−silica material revealed a type IVb BET isotherm with a large hysteresis, commonly due to network penetration effects.[36] Judging from this hysteresis, the material most likely contains a wormhole-like porous structure. The surface area was 588.2 m^2 g^{-1}, with a broad BJH pore size distribution and a median pore diameter of 75.1 Å as shown in Figure 3**.** We note that the pore size of our material is larger than those of the uranyl-exchanged MCM-41/MCM-48 mesoporous silica analogues, which typically have pore diameters of around 1−3 nm.[30,32] The pore size distribution of MCM-41 is generally narrower than that seen in Figure 3 for the $U_{aq}O_2^{2+}$−silica catalyst. Interestingly, in contrast to the surface areas (around 250−300 m^2 g^{-1}) of the literature-reported SDS-templated mesoporous silica materials,[37] our mesoporous $U_{aq}O_2^{2+}$−silica catalyst exhibits a significantly larger surface area, considering that the surfactant remains inside the pores. We attribute this large surface area to the unique templating method, where the uranyl ions play a key role in altering the porous silica structure, as demonstrated previously in uranyl-derivatized zeolite and MCM-48 systems.[22,32] The unique templating method utilized here results in an electrostatic interaction where the uranyl ions are located beyond the scope of the surfactant micelle, thereby increasing the average pore diameter of the silicate, which condenses around it.

SEM studies of these hybrid materials revealed amorphous to spherical morphologies of approximately 1 μm in diameter. The surface of the material appears rough, and the particles aggregate notably. In some areas, the semispherical morphologies appear fused, as depicted in Figure 4a. TEM micrographs showed a wormhole-like porous structure as illustrated in Figure 4b, which confirmed the observation in the surface sorption BET studies.

The uranium content of $U_{aq}O_2^{2+}$−silica was determined by two independent methods. In one, the silica matrix was dissolved in concentrated acid and the uranium content was quantified by inductively coupled plasma mass spectrometry (ICP-MS). The material was first treated with *Aqua Regia*, and after approximately 2 h of stirring, the silica component was dissolved by the addition of 40% hydrofluoric acid. The solution was stirred for 12 h, diluted, and tested for uranium content using a thorium internal standard. Another sample of $U_{aq}O_2^{2+}$−silica was stirred in 1 M H_3PO_4 for several hours. After filtration, the concentration of $U_{aq}O_2^{2+}$ in solution was determined spectrophotometrically (λ = 421 nm, ϵ = 17.7 M^{-1} cm^{-1}). The agreement between the two methods was excellent, 4.30% vs 4.36% U by weight.

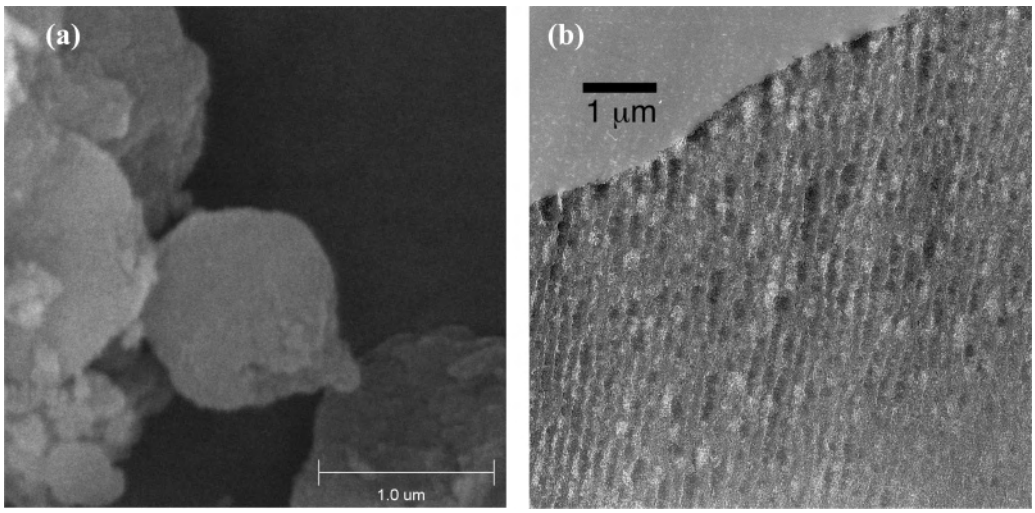

Figure 4. (a) SEM micrograph and (b) TEM micrograph of the $U_{aq}O_2^{2+}$−silica material.

Table 1. Summary of Kinetic Data ($k_Q/M^{-1}\ s^{-1}$) for the Quenching of Excited-State Uranyl Ions with Alcohols

substrate	$U_{aq}O_2^{2+}/H_3PO_4$[a]	$U_{aq}O_2^{2+}/H_2O$[b]	$U_{aq}O_2^{2+}$[c]	$U_{aq}O_2^{2+}-$silica[d-f]	$U_{aq}O_2^{2+} + SiO_2$[c,g]
MeOH	1.5×10^6[h]	6.4×10^6		7.3×10^5	
2-PrOH	1.4×10^7[h]	8.5×10^7	3.1×10^5	1.3×10^7	1.7×10^5
2-BuOH	1.7×10^7			1.7×10^7	
2-pentanol	1.8×10^7			1.5×10^7	
t-BuOH	1.4×10^5			1.2×10^5	
none[i]	1.0×10^4	8.3×10^5	4.0×10^4	1.5×10^4	3.7×10^4

[a] 0.6 M aqueous H_3PO_4. [b] In water at natural pH (~7). Data from ref 39. [c] In water + 1.0 mM NaOH added. U content: 0.6 mM. Measured pH = 5. [d] 1 mM NaOH added. Measured pH ~ 5; see text. [e] $U_{aq}O_2^{2+}$ on mesoporous silica. [f] At [alcohol] ≤ 15 mM, see text. [g] Aqueous $U_{aq}O_2^{2+}$ + silica gel. [h] Data from ref 17. [i] Self-decay rate constants in units of s^{-1}.

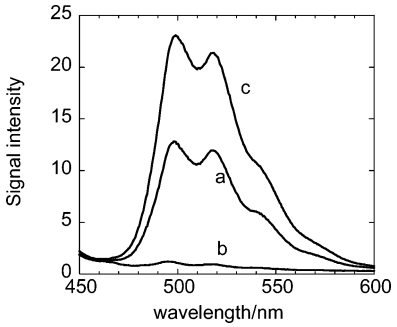

Figure 5. (a) Emission spectrum of 10 mg of $U_{aq}O_2^{2+}-SiO_2$ (1.8 μmol of $U_{aq}O_2^{2+}$) in 3 mL of water. (b) After acidification of sample a with $HClO_4$ to pH 2. (c) After neutralization of sample b with NaOH (pH ~5).

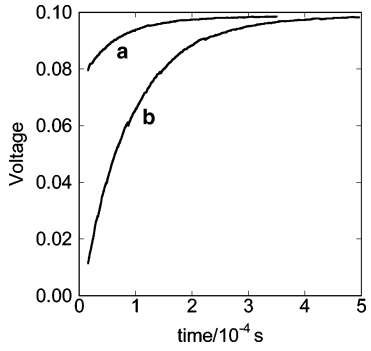

Figure 6. (a) Luminescence decay for a suspension of $U_{aq}O_2^{2+}-SiO_2$ in water (pH ~5). (b) After the addition of NaOH to sample a, added $[OH^-] = 1$ mM. The measured pH for both samples was ~5; see text.

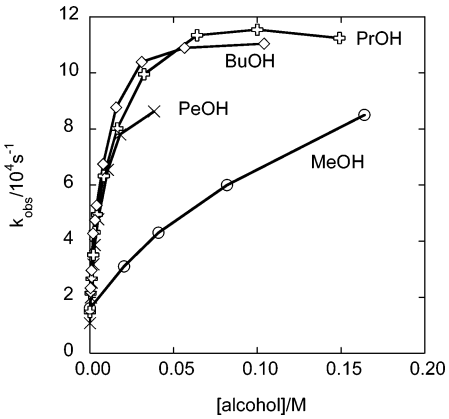

Figure 7. Plot of k_{obs} vs alcohol concentration for the quenching of $*U_{aq}O_2^{2+}-$silica by 2-PrOH (pluses), 2-BuOH (diamonds), 2-pentanol (crosses), and MeOH (circles).

Quenching Kinetics. The intensity of the emission spectrum of a sample containing 10 mg of $U_{aq}O_2^{2+}-SiO_2$ (1.8 μmol of $U_{aq}O_2^{2+}$) in 3 mL of water decreased dramatically when the solution was acidified with $HClO_4$ or H_3PO_4 to pH 2 **(**Figure 5). The emission was restored upon the addition of 1 equiv of NaOH.

Time-resolved emission was monitored at 515 nm in laser flash photolysis experiments. The first 15 μs in all of the kinetic traces in this work had to be discarded because a large signal, believed to be an artifact caused by light scattering in these nonhomogeneous samples, obscured the fluorescence on this time scale.

Lifetime determinations were carried out on suspensions of $U_{aq}O_2^{2+}-SiO_2$ in water, which exhibited a natural pH of ~5. For some samples, sufficient 0.10 M NaOH was added to make $[OH^-] = 1$ mM. The measured pH for such samples was also ~5. Clearly, the added NaOH was neutralized by either the acidic sites on silica ($pK_a \sim 4-7$ for surface silanol groups[38]), coordinated water[28] on $U_{aq}O_2^{2+}$, or both. The amplitude of the voltage vs time trace for emission decay at 515 nm (Figure 6) was much greater for the partly neutralized sample, but the decay rate ($1.2 \times 10^4\ s^{-1}$) was close to that observed for the untreated sample ($1.6 \times 10^4\ s^{-1}$).

The quenching of $*U_{aq}O_2^{2+}-$silica by alcohols, eq 1, exhibited exponential kinetics, but the plot of k_{obs} against the alcohol concentration saturates at high alcohol concentrations (Figure 7). From the data at low alcohol concentrations, the lower limits of the second-order rate constants were calculated and listed in Table 1.

$$*U_{aq}O_2^{2+}-\text{silica} + \text{alcohol} \rightarrow \text{products} \qquad k_Q \qquad (1)$$

Isotope Effects. The quenching of $*U_{aq}O_2^{2+}$ with $CD(CD_3)_2OH$ in H_2O is slower than that with the protio compound at low alcohol concentrations, i.e., those describing the curved portion of the k_{obs} vs [2-PrOH] plot. In the saturation regime, however, the two rate constants are comparable, as shown in Figure 8. The data shown have been corrected for the self-decay of $*U_{aq}O_2^{2+}$, $k_0 = 1.48 \times 10^4\ s^{-1}$. In the concentration range examined, the kinetic isotope effect (kie), expressed as k_H/k_D, decreased smoothly from 2.0 at the lowest alcohol concentration to 1.0 at the highest concentration.

(36) Rouquerol, F.; Rouquerol, J.; Sing, K. *Absorption by Powders & Porous Solids. Principles, Methodology, and Applications*; Academic Press: New York, 1999; p 440.
(37) Yokoi, T.; Yoshitake, H.; Tatsumi, T. *Chem. Mater.* **2003**, *15*, 4536−4538.
(38) (a) Rouxhet, P. G.; Sempels, R. E. *J. Chem. Soc., Faraday Trans. 1* **1974**, *70*, 2021−2032. (b) Dorsey, J. G.; Cooper, W. T. *Anal. Chem.* **1994**, *66*, 857A. (c) Mendez, A.; Bosch, E.; Roses, M.; Neue, U. D. *J. Chromatogr. A* **2003**, *986*, 33.

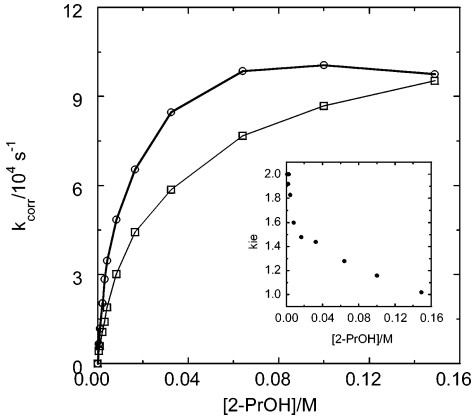

Figure 8. Plot of the rate constants for the quenching of $*U_{aq}O_2^{2+}-SiO_2$ by $CH(CH_3)_2OH$ (top) and $CD(CD_3)_2OH$ (bottom). The data were corrected for the self-decay path, $k_0 = 1.48 \times 10^4\ s^{-1}$. The inset shows the variation of the kinetic isotope effect with the concentration of 2-PrOH.

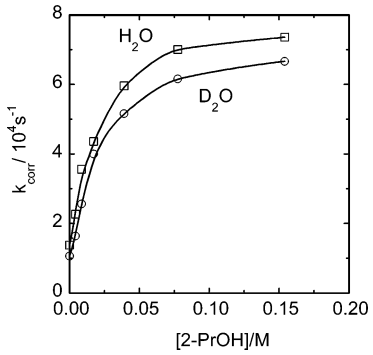

Figure 9. Plot of k_{corr} for the quenching of $*U_{aq}O_2^{2+}-SiO_2$ by 2-PrOH in H_2O (top) and 2-PrOD in D_2O (bottom).

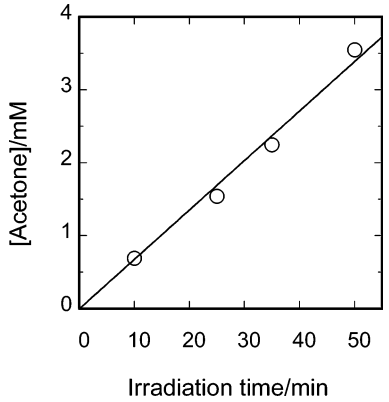

Figure 10. Yields of acetone as a function of the irradiation time for the reaction of 2-PrOH with mesoporous $*U_{aq}O_2^{2+}-SiO_2$. Conditions: [2-PrOH] = 87 mM; 20 mg of $U_{aq}O_2^{2+}-SiO_2$ (3.6 μmol of $U_{aq}O_2^{2+}$) in 3 mL of D_2O (pH 5).

The solvent isotope effect for the quenching of $*U_{aq}O_2^{2+}-SiO_2$ by 2-PrOH is close to unity, as shown in Figure 9. Throughout the range of concentrations examined, the curves for H_2O and D_2O are approximately parallel, with the values in H_2O being somewhat larger than those in D_2O.

Products. Steady-state photolysis of $U_{aq}O_2^{2+}$−silica in D_2O-containing $CH(CH_3)_2OH$ produced acetone, as determined by ^1H NMR. The yield of acetone increased linearly with the irradiation time (Figure 10) and somewhat with the amount of $U_{aq}O_2^{2+}$−silica used. Small amounts of base had a beneficial effect, but the yields peaked at 4 mM added OH^- (still giving a measured pH of ∼7) and then decreased rapidly at higher base concentrations.

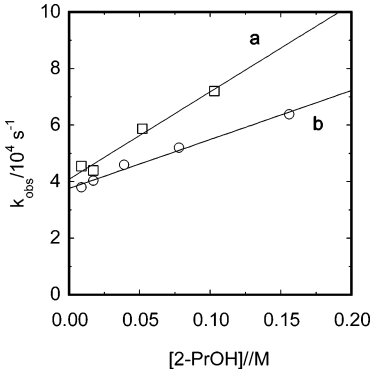

Figure 11. Plot of k_{obs} vs concentration of 2-PrOH for the reaction of 2-PrOH with (a) aqueous $*U_{aq}O_2^{2+}$ and (b) $*U_{aq}O_2^{2+}$−silica gel mixtures.

After 50 min of photolysis, a sample containing 20 mg of $U_{aq}O_2^{2+}$−silica (3.6 μmol of $U_{aq}O_2^{2+}$) in 3 mL of 87 mM 2-PrOH produced 11 μmol of acetone, demonstrating that the reaction is catalytic in $U_{aq}O_2^{2+}$. Moreover, from the linear plot in Figure 10, we expect that a much larger turnover number would have been reached after longer times.

Under identical conditions, 2-butanol (2-BuOH; 87 mM) yielded 6 μmol of 2-butanone and 2-pentanol (87 mM) yielded 5 μmol of 2-pentanone. The smaller yields of these ketones compared to acetone, despite the larger quenching rate constant for 2-pentanol (and, presumably, for 2-BuOH as well), suggest that static quenching may be contributing to the loss of the excited state. Such a pathway has been reported previously in the reaction between ethanol and $*U_{aq}O_2^{2+}$ on colloidal silica.[19] It is also possible that the presence of reasonably reactive methylene hydrogens in 2-BuOH and 2-pentanol, but not in 2-PrOH, diverts some of the excited state from methine hydrogens, resulting in smaller yields of the ketones. In fact, these additional reactive C−H bonds may be responsible for faster quenching. However, the NMR spectra provided no evidence for products derived from the oxidation of methylene groups.

Reactions of $U_{aq}O_2^{2+}$ Adsorbed on Silica Gel. For these experiments, the amounts of both silica and uranium were the same as those in kinetic experiments with the mesoporous material. Typically, 10 mg of silica gel was added to a solution containing 0.6 mM uranyl nitrate in water. The suspension was shaken and treated with a small amount of NaOH (measured pH ∼5). The lifetime of $*U_{aq}O_2^{2+}$ was somewhat shorter than that for the mesoporous samples (Table 1).

The quenching with 2-PrOH yielded exponential traces. The dependence of k_{obs} on the concentration of 2-PrOH is almost linear and gives $k = 1.7 \times 10^5\ M^{-1}\ s^{-1}$, although the data may indicate a slight downward trend at the highest [2-PrOH] (Figure 11).

Reactions of Homogeneous $*U_{aq}O_2^{2+}$. Aqueous solutions of $U_{aq}O_2^{2+}$ in the absence of SiO_2 were treated with NaOH in the same manner as the SiO_2 suspensions above. Qualitatively, the kinetic behavior was the same as that exhibited by mixtures of $U_{aq}O_2^{2+}$ and silica gel and yielded $k_0 = 4.0 \times 10^4\ s^{-1}$ (pH 5). The quenching with 2-PrOH exhibited a

linear dependence of k_{obs} on [2-PrOH] and yielded $k_{2-PrOH} = 3.1 \times 10^5\ M^{-1}\ s^{-1}$. All of the kinetic data are summarized in Table 1.

Tests for $U_{aq}O_2^{2+}$ Leaching. The kinetic behavior of the mesoporous $U_{aq}O_2^{2+}-SiO_2$ is clearly different from those of homogeneous solutions of $U_{aq}O_2^{2+}$ or the $U_{aq}O_2^{2+}$−silica gel mixtures. This result already establishes that $U_{aq}O_2^{2+}$ is not readily leached from the mesoporous material in the absence of acid. This result was confirmed by suspending $U_{aq}O_2^{2+}-SiO_2$ in H_2O and then separating the solid and solution phases by centrifugation and filtration. The filtrate ("filtrate-1") exhibited a weak luminescence. The solid ("solid-1") was resuspended in H_2O to make "sample-2" and also exposed to a laser shot. The size of the signal was somewhat (∼20%) smaller than that for the original sample. Clearly, some $U_{aq}O_2^{2+}$ had been transferred into the solution phase. The procedure was repeated one more time by centrifugation/filtration of "sample-2" and resuspension. This time all of the luminescence was associated with the solid. We interpret these data to mean that some free $U_{aq}O_2^{2+}$ had been present initially in our sample of $U_{aq}O_2^{2+}-SiO_2$. Once removed, no additional uranium was leached from the solid.

Additional experiments were carried out to determine whether any $U_{aq}O_2^{2+}$ was lost from the support during prolonged photolysis times. A sample initially containing 20 mg of $U_{aq}O_2^{2+}-SiO_2$ in 3 mL of 2 mM NaOD in D_2O (final pH 5) was centrifuged, and the solid and solution were tested separately for their catalytic activities. The solid was resuspended in 3 mL of D_2O/NaOD containing 87 mM 2-PrOH, and the sample was photolyzed for 50 min. The yield of acetone was 7 μmol (2.35 mM), showing that a significant amount of $U_{aq}O_2^{2+}$ was still present in the sample. Admittedly, the amount of acetone was smaller than that in an otherwise identical experiment where the removal and resuspension steps were omitted (11 μmol, 3.7 mM). The reduced yield is believed to be caused by the loss of the solid catalyst during the manipulations of the small-size sample and not by leaching. In support of this proposal, the solution from the centrifuged sample had no measurable catalytic activity.

Mineral acids ($HClO_4$, H_3PO_4) readily leach $U_{aq}O_2^{2+}$ from $U_{aq}O_2^{2+}-SiO_2$. This was shown in experiments similar to those described above except that solutions were acidic (0.01−0.1 M $HClO_4$ or H_3PO_4). In every case, all of the luminescence was associated with the solution phase, and none remained with the solid material.

Stability of Uranium Samples. The kinetic behavior of all of the samples (homogeneous aqueous solutions, suspensions of $U_{aq}O_2^{2+}$−silica in water with or without the treatment with NaOH, and $U_{aq}O_2^{2+}$−silica gel mixtures) was checked for freshly prepared samples and again after the samples were allowed to age for 2 h. Within the experimental error, the rate constants and signal sizes remained unaffected during the aging time.

Discussion

Unlike the previously reported base-catalyzed syntheses,[29,32] where multiple uranium oxide species were often observed because of the undesirable polymerization of uranyl ions, the synthesis of our $U_{aq}O_2^{2+}$−silica material is based on an acid-catalyzed co-condensation reaction. Under the acidic condition, the surfactant is negatively charged (I^-), uranium(VI) is present as $U_{aq}O_2^{2+}$ (M^+), and the silicate was condensed around these ionic species in situ. The structure of the resulting $U_{aq}O_2^{2+}$−silica material can be further stabilized by extensive washing with water and MeOH to deprotonate the silanol groups and to establish the desired $I^-M^+S^-$ electrostatic interactions. This strong electrostatic interaction between the surfactant, silica, and uranyl ions yielded a stable material, which did not require calcination for the adhesion of the uranyl ions to the silica surface. Throughout our investigation, no leaching of the uranyl ions was observed.

The single-exponential decay of $*U_{aq}O_2^{2+}$−silica in the absence of added substrates (Figure 6) suggests that there is only one kind of uranium present in the material. Because the synthesis was carried out under acidic conditions where monomeric aqua species dominate, the uranium ions in silica−$U_{aq}O_2^{2+}$ are probably also monomeric. The kinetic data also suggest that all of the uranium ions have the same coordination environment and are situated in similar (identical?) crystallographic sites. This result differs from the observations on uranyl ions supported on colloidal silica,[19,27] zeolites,[20−23] and clays.[22,24] In those cases, the decay kinetics obeyed double- and, sometimes, triple-exponential rate laws, suggesting the presence of both monomeric and dimeric species[20] and different coordination and crystallographic sites.[22,24] On the other hand, uranyl-doped sol−gel glasses, prepared under acidic conditions,[26] decayed by first-order kinetics and had a luminescence spectrum indicative of a monomeric uranyl.

Hydroxide affects greatly the intensity of uranyl luminescence (Figure 5). Almost certainly, uranyl hydrolysis is responsible for at least some of this effect, as was shown to be the case in a homogeneous aqueous solution.[19] We suggest, however, that the silica support plays a role too. Uranyl hydrolysis should be limited to the loss of hydrogen ions from coordinated molecules of water, but the dimerization comparable to that in solution[28] is ruled out by the nature of supported species. Partly deprotonated silica surface may, however, play a role similar to that of hydroxo bridges in a homogeneous solution.

The effect of hydroxide on the luminescence intensity, but not on the rate of excited-state decay (Figures 5 and 6), suggests that the same (or similar) excited uranium species is responsible for luminescence in both cases, although the ground-state species is almost certainly different in the two samples, as judged by the more intense yellow color of the solid and higher concentration of the excited state for the partially neutralized material. Apparently, the acid/base chemistry of the excited state is fast on the time scale of excited-state decay. Thus, the addition of hydroxide changes the yield but has only a minor, if any, effect on the chemical composition or hydrolytic state of the observed excited state.

Reactivity of $*U_{aq}O_2^{2+}$−Silica. The formation of ketones from secondary alcohols establishes that the quenching takes

place, at least in part, by a chemical mechanism, most likely by hydrogen abstraction followed by rapid oxidation of the radicals by O_2 and/or $U_{aq}O_2^{2+}$, as established in a homogeneous solution.[14,15,17] The kinetics of individual steps (hydrogen abstraction, oxidation of radicals to products, and reoxidation of $U_{aq}O_2^{+}$) have not been determined for the supported material, but there is no loss of activity after three catalytic cycles (Figure 10). Thus, all of the steps are efficiently keeping up with the quenching rates displayed in Figure 7.

The reaction with *t*-BuOH produced small amounts of acetone, suggesting some hydrogen abstraction from the OH group followed by β scission of the resulting alkoxyl radicals. A similar proposal has been put forward for the solution reaction,[2] although the isotope effect for the hydroxo group did not seem to support such a mechanism, $k_{OH}/k_{OD} = 0.94$.[17]

The quenching of $*U_{aq}O_2^{2+}$−silica by alcohols is a complex process, as shown by the saturation kinetics in Figure 7. Even more peculiar is the concentration-dependent kie in Figure 8. In the low-concentration regime, the value of k_H/k_D is 2.0, somewhat smaller than that observed in homogeneous solutions[17,39] for which quenching by hydrogen abstraction is well established. In the saturation regime, the isotope effect mostly disappears, indicating a change in the rate-limiting step. We suggest that diffusion of the substrate to the excited state becomes slow relative to hydrogen abstraction at high [alcohol]. Even though the pores in mesoporous silica are large, the encapsulated surfactant molecules may slow the diffusion of reactant/product molecules through the channels. The idea of limiting diffusion is supported by the similarity in rate constants for all of the alcohols in the plateau range, despite the significant difference in the bimolecular rate constants between MeOH and secondary alcohols at low alcohol concentrations.

A comparison of the oxidation abilities of various $U_{aq}O_2^{2+}$-based catalysts is shown in Table 1. The quenching rate constants are the largest in neutral homogeneous solutions, but the short lifetime of $*U_{aq}O_2^{2+}$ ($\sim$1 μs) limits catalysis to high substrate concentrations. The somewhat lower reactivity in the presence of H_3PO_4 is more than offset by the almost 100-fold increase in the lifetime of the excited state (100 μs). Of all of the cases in Table 1, this one provides the best conditions for substrate oxidation. The addition of small amounts of NaOH to aqueous solutions of uranyl decreases the reactivity but increases the signal size (about 5-fold) and the lifetime of the excited state, both of which have a positive effect on the product yield.

$U_{aq}O_2^{2+}$−silica compares favorably with other cases, including the homogeneous $U_{aq}O_2^{2+}/H_3PO_4$ catalyst. Both the lifetimes and the reactivities at low alcohol concentrations are almost identical for the two. This result is particularly impressive in view of the much lower reactivity of silica gel supported uranyl, which reacts with 2-PrOH almost 100 times more slowly than the mesoporous material does. Because the two materials are chemically identical, it is clear that the structure of the mesoporous material plays a major role. The reason for the greater reactivity of the mesoporous material could be the large diameter of the channels, allowing the reductant an unimpeded approach to the uranium, or some more subtle structural detail or distribution of uranium ions on the support.

At higher substrate concentrations, the supported material exhibits kinetic saturation, which makes it less reactive than the homogeneous $U_{aq}O_2^{2+}/H_3PO_4$ catalyst. Still, even in the plateau region, the oxidation is efficient and only about 15% of the excited state is lost by self-decay.

The oxidation efficiency of $U_{aq}O_2^{2+}$−silica stands in strong contrast to the inferior behavior of $U_{aq}O_2^{2+}$−silica gel mixtures (last column in Table 1) in terms of both the lifetime and reactivity. In fact, silica gel appears to offer only a minimal, if any, advantage over purely aqueous solutions that have undergone identical treatment prior to the oxidation experiment, columns 4 and 6 in Table 1, suggesting that perhaps most of the uranyl ions are not associated with silica. This behavior is different from the greatly extended lifetimes of the uranyl ions in colloidal silica solutions.[19]

If the goal of heterogeneous catalysis is to achieve the reactivity and selectivity of the homogeneous catalysts, then the results obtained in this work are encouraging. In addition, the mesoporous $U_{aq}O_2^{2+}$−silica appears resistant to leaching by neutral or alkaline water, even after prolonged reaction times. Similar to the aqueous species,[17] the supported catalyst is more selective and yields fewer products than is normally seen in free-radical reactions. The similarity in chemistry extends to uranyl(V) as well. The association with the silica surface obviously did not cause a significant rate decrease for the $U_{aq}O_2^{+}/O_2$ reaction, which is only moderately fast in aqueous solutions ($k = 31.4\ M^{-1}\ s^{-1}$).[18]

Acknowledgment. Support for this research was provided by the U.S. Department of Energy, Office of Basic Energy Sciences, through Catalysis Science Grant AL 03 380 011 and by the DOE Center for Catalysis, Iowa State University (Contract DEFG0202ER63371-CCAT-KR). The authors thank C. T. Gross and Professor R. S. Houk for their assistance in ICP-MS measurements.

IC050130E

(39) Hill, R. J.; Kemp, T. J.; Allen, D. M.; Cox, A. *J. Chem. Soc., Faraday Trans. 1* **1974**, *70*, 847−857.